Title
LOW-FREQUENCY WAVES IN A WEAKLY IONIZED, ROTATING MAGNETOPLASMA

Authors
Wheeler, George M.
Pyle, Robert V.

Publication Date
1973-04-01

Submitted to
Physics of Fluids

LBL-1785
Preprint c.1

LOW-FREQUENCY WAVES IN A WEAKLY IONIZED, ROTATING MAGNETOPLASMA

George M. Wheeler and Robert V. Pyle

April 1973

Prepared for the U. S. Atomic Energy Commission
under Contract W-7405-ENG-48

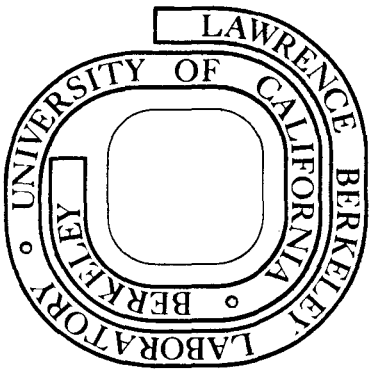

DISCLAIMER

LOW-FREQUENCY WAVES IN A WEAKLY IONIZED, ROTATING MAGNETOPLASMA

George M. Wheeler* and Robert V. Pyle

Lawrence Berkeley Laboratory
University of California
Berkeley, California 94720

ABSTRACT

A single-fluid theory is developed which explains the experimental behavior of a low-frequency (~ 2 kHz) flute instability in a hollow cathode discharge (HCD) plasma. The effects of density gradient, centrifugal and Coriolis forces due to plasma rotation in a nonuniform, radial electric field, and ion-neutral collisions are included in a linear fluid theory. A cubic dispersion equation results which is solved numerically using experimental plasma profiles. In the low-frequency limit ($\omega/\Omega_i << 1$), the dispersion relation reduces to a quadratic expression which is consistent with earlier work in the appropriate limits. Collisions are found to be stabilizing, while the Coriolis effect depends on the direction of plasma rotation. The theory is able to predict, within experimental uncertainty, the frequencies observed in two similar experiments.

I. INTRODUCTION

The existence of a gravitational-type plasma instability was shown theoretically nearly 20 years ago by Kruskal and Schwarzchild.[1] Since then the theory has been expanded and improved by many authors, but only recently has the instability been observed experimentally. A convenient experiment for studying this effect makes use of a rotating cylindrical plasma. In this case, the centrifugal force is the experimental analog to gravity, and one could expect instability if a density gradient exists antiparallel to the centrifugal force.

A magnetized hollow cathode discharge (HCD) provides a suitable experimental plasma, which is usually rotating in a radial electric field. A strong radial density gradient also exists across an axial magnetic field. Under these conditions, it is not surprising that the $\underline{E} \times \underline{B}$ neutral drag instability[2] and the resistive drift instability[3-5] have been "identified" in an HCD. Also, the electrostatic ion cyclotron instability[5] and the ion-acoustic instability[6] have been reported. However, the theories for these instabilities seem incomplete in not including all of the important effects simultaneously. In addition, the resistive drift instability requires finite parallel wavelength, which is rarely observed in an HCD.

In 1969, Hudis first "identified" a Rayleigh-Taylor centrifugal flute instability in an HCD by comparing the measured frequency with a calculated value.[7] He used a slab model and pointed out that the important effect of the Coriolis force was missing. More recently the problem has been solved numerically for a collisionless plasma in cylindrical geometry by Ilić et al.[8] They solved for the perturbed eigenfunctions

and eigenfrequencies using plasma profiles similar to their experimental values.

In the present work, we choose an analytic approach and include the effects of centrifugal and Coriolis forces, ion-neutral collisions, ion inertia, and finite ion gyroradius (FGR) in a slab fluid model. The theory is compared with data from the present experiment, and with measurements of Hudis[7] and Ilić et al.[8]

II. THEORY

Most theories developed for a centrifugal instability seem incomplete, particularly when applied to an HCD, which contains several important destabilizing mechanisms. A consistent theory should take geometry into account. For the special case of uniform plasma rotation one obtains Whittaker's equation.[9] (However, quantization of the radial mode number makes the results difficult to interpret.)

For the more realistic case of nonuniform rotation, no known analytic solution exists. In this case, one can integrate the fluid equations numerically over the radial profiles and apply radial boundary conditions to obtain both the eigenfrequencies and eigenfunctions of the normal modes. Ilić et al. have used this numerical technique for a collisionless plasma, to obtain fair agreement with experiment.[8]

Roberts and Taylor presented a simple and useful fluid derivation of the centrifugal instability in slab geometry which correctly included the effects of finite ion gyroradius (FGR) and ion inertia.[10] However, they neglected the effects of the Coriolis force and ion-neutral collisions which are important in an HCD. Lehnert introduced the Coriolis force into the fluid equations in a slab geometry, but collisions were still neglected.[11]

In this work we modify the derivation of Roberts and Taylor to include ion-neutral collisions, and introduce centrifugal and Coriolis forces in a slab geometry. The use of slab geometry is a valid simplification at sufficiently large radii that the radius is much larger than the radial scale length of plasma parameters q, or $q << R$. It also allows us an analytic solution.

We write down a familiar form of the single fluid equations using e. m. u:

$$\rho \frac{d\underline{v}}{dt} \equiv \rho \dot{\underline{v}} = \rho_e \underline{E} + \underline{j} \times \underline{B} - \nabla p - \nabla \cdot \underline{\underline{P}} + \underline{F} - \rho \nu_{in} \underline{v} \tag{1}$$

$$\frac{\partial \rho}{\partial t} + \nabla \cdot (\rho \underline{v}) = 0 \tag{2}$$

$$\frac{m}{ne^2} \frac{d\underline{j}}{dt} = \underline{E} + (\underline{v} - \underline{j}/ne) \times \underline{B} + \frac{\nabla p_e}{ne} - \eta \underline{j} . \tag{3}$$

We define the following symbols: $\Omega_\alpha = e_\alpha B/m_\alpha c$ is the cyclotron frequency; $\nu_{\alpha n}$ is the collision frequency for species α with neutrals; $a_i \equiv v_t^i/\Omega_i$ is the ion gyroradius; $\nu \equiv a_i^2 \Omega_i/4$ is the collisionless viscosity; $\delta \equiv q^{-1} \equiv - \nabla \ell n\, n(x)$ is the assumed constant inverse density scale length; $\underline{\Omega}_0 \equiv \Omega_0 \hat{z}$ is the assumed uniform plasma rotation frequency; $\underline{g} \equiv g \hat{x}$ is the effective centrifugal gravity; and $\nabla \cdot \underline{\underline{P}} \equiv - \nu \underline{\lambda}$ is the divergence of the collisionless pressure tensor. The components of $\underline{\lambda}$ can be written:[10, 12]

$$\lambda_x = \partial/\partial x[\rho(\partial v_y/\partial x + \partial v_x/\partial y)] - \partial/\partial y[\rho(\partial v_x/\partial x - \partial v_y/\partial y)]$$

$$\lambda_y = - \partial/\partial y[\rho(\partial v_y/\partial x + \partial v_x/\partial y)] - \partial/\partial x[\rho(\partial v_x/\partial x - \partial v_y/\partial y)] .$$

We assume: (1) quasi-neutrality, $\rho_e = 0$; (2) neglect of electron inertia, $\partial E/\partial t = \partial j/\partial t = 0$; (3) negligible resistivity, $\eta = 0$; (4) low β; (5) axial uniformity, $\partial/\partial z = 0$; (6) plasma slowly varying with respect to ion gyroradius, ka_i, $\delta a_i << 1$; (7) negligible temperature gradient effects; and (8) centrifugal and Coriolis forces, $\underline{F} \equiv \rho \underline{g} + 2\rho \underline{v} \times \underline{\Omega}_0$.

With these assumptions Eqs. (1) and (3) reduce to:

$$\rho \dot{\underline{v}} = \underline{j} \times \underline{B} - \nabla p + \nu \underline{\lambda} + \rho \underline{g} + 2\rho \underline{v} \times \underline{\Omega}_0 - \rho \nu_{in} \underline{v} \tag{4}$$

$$\underline{E} + \underline{v} \times \underline{B} = \underline{j}/ne \times \underline{B} - \nabla p_e/ne. \tag{5}$$

The solution is obtained by linearizing Eqs. (2), (4), and (5), assuming first-order quantities of the form, $\exp[i(ky-\omega t)]$. However, in Eq. (4) the ion-neutral collision frequency, ν_{in}, is combined with the time derivative to yield an effective frequency, $\omega' = \omega + i\nu_{in}$. The Coriolis term is combined with the Lorentz force term to yield an effective magnetic field, $\underline{B}^* \equiv \underline{B} + 2\rho\underline{\Omega}_0/ne = \underline{B}(1 + 2\Omega_0/\Omega_i) \equiv \underline{B}\Lambda$.

A cubic dispersion relation results,

$$\omega'^3 \left(\frac{\delta}{k\Omega_i}\right) - \omega'^2 \left(1 + i\,\frac{\delta \nu_{in}}{k\Omega_i}\right) + \omega' \left(\frac{kg}{\Omega_i} + 2\nu\delta k\Lambda - \frac{2\Omega_0 \delta\Lambda}{k} + i\nu_{in}\right)$$

$$- g\delta\Lambda - i\nu_{in}\Lambda(2\nu\delta k - 2\Omega_0\delta/k) = 0. \tag{6}$$

The cubic term is of the order of ω/Ω_i and may be neglected for low frequencies $(\omega/\Omega_i << 1)$ in order to compare our results with earlier work. If we also neglect collisions, $\nu_{in} = 0$, we get

$$\omega^2 - \omega \left(\frac{kg}{\Omega_i} + 2\nu\delta k\Lambda - \frac{2\Omega_0\delta\Lambda}{k}\right) + g\delta\Lambda = 0. \tag{7}$$

The first term in the coefficient of ω is the usual gravitational effect, the second term shows the effect of finite ion gyroradius (FGR), and the third term is the contribution due to the Coriolis force, which introduces the asymmetry in the frequency and stability condition depending on the direction of plasma rotation. Note that in Eq. (7) the Coriolis force can be either stabilizing or destabilizing, depending on the direction of plasma rotation, Ω_0 .[13]

If we neglect the Coriolis term, this is exactly the result of Roberts and Taylor. If we neglect FGR effects and the Coriolis force term, our result reduces to the earlier work of Lehnert.[14] Neglecting only FGR effects, $\nu = 0$, our result reduces to Lehnert's work with the Coriolis force included.[11]

The effect of ion-neutral collisions is difficult to predict analytically, since we must break the complex dispersion relation into real and imaginary parts. By varying the collision frequency in the cubic dispersion relation, and solving numerically, we find that collisions are stabilizing, in agreement with earlier work.[13,15]

A. Phase Relations

We can also calculate how much the phase between the density and potential fluctuations is shifted due to collisions and the Coriolis force. The mathematics can be simplified considerably by solving the ion moment equations as a function of frequency, and using the complex frequency from the dispersion relation, Eq. (6).

We write down the equations of motion and conservation for the ions:

$$n_i M_i \dot{\underline{v}}_i = n_i e(\underline{E} + \underline{v}_i \times \underline{B}) - kT_i \nabla n_i + n_i M_i \underline{g} + 2 n_i M_i \underline{v}_i \times \underline{\Omega}_0 - n_i M_i \nu_{in} \underline{v}_i \qquad (8)$$

$$\dot{n}_i + \nabla \cdot (n_i \underline{v}_i) = 0, \qquad (9)$$

where $\underline{\Omega}_0 = \Omega_0 \hat{z}$ is the azimuthal plasma rotation frequency.

Consider the zero-order, steady-state form of Eq. (8) in the drift frame, where $\underline{v}_0 = 0$,

$$e\underline{E}_0 - kT_i \frac{\nabla n_0}{n_0} + M_i \underline{g} = 0. \tag{10}$$

If we linearize Eqs. (8) and (9), assuming electrostatic fluctuations, we get the required phase relation,

$$\frac{\tilde{n}}{\tilde{\phi}} = \frac{kv_{De}}{\Lambda\omega} \frac{1 - \alpha k/\delta}{1 - \alpha^2} \tag{11}$$

where $\alpha \equiv \omega'/\Lambda\Omega_i$, $\tilde{n} \equiv n_1/n_0$, $\tilde{\phi} \equiv e\phi_1/kT_e$, and $v_{De} \equiv kT_e\delta/eB$ is the electron diamagnetic velocity.

For low frequencies, growth rates, and collision frequencies, $|\alpha| << 1$, we get a simple relation,

$$\frac{\tilde{n}}{\tilde{\phi}} \approx \frac{kv_{De}}{\Lambda\omega}, \quad |\alpha| << 1. \tag{12}$$

If, on the other hand, the collision frequency is so large that $\alpha = i\nu_{in}/\Omega_i\Lambda >> 1$, then Eq. (11) becomes

$$\frac{\tilde{n}}{\tilde{\phi}} \approx -i \frac{kv_{De}}{\omega} \frac{k}{\delta} \frac{\Omega_i}{\nu_{in}}, \quad |\alpha| >> 1. \tag{13}$$

When collisions and the Coriolis force are unimportant ($|\alpha| << 1$), the phase between the density and potential fluctuations agrees with a simple picture presented by Chen.[16] But when collisions and Coriolis force are important ($|\alpha| >> 1$), the phase can be shifted by up to 90°. The measured phase lies somewhere between the two. (This fact is useful in estimating enhanced convection correctly.)

B. Electric Field

The ion equation of motion can also be solved for the steady-state radial electric field in terms of the plasma rotation velocity and the gravitational and diamagnetic drifts. The plasma rotation velocity can be measured directly using a directional Langmuir probe, from which the centrifugal gravity, $g = V_\theta^2/r$, and the Coriolis force, $\underline{F}_c = 2M\underline{v} \times \underline{\Omega}_\theta$, can be inferred. A useful expression for E_r results:

$$E_r = -\frac{B}{e}\left[V_\theta \Lambda \left(1 + \frac{\nu_{in}^2}{\Omega_i^2 \Lambda^2}\right) + \frac{g}{\Omega_i} - \frac{kT_i}{eB}\frac{c\nabla n}{n}\right]. \qquad (14)$$

III. EXPERIMENTAL ARRANGEMENT

The present experiment was conducted in the partially ionized plasma surrounding a hollow cathode discharge, the properties of which are discussed in detail in the literature.[17,18] The experimental arrangement is shown in Fig. 1, except that anode A_I was not used in this experiment. An axial magnetic field, supplied by six modular coils, was varied from 580 to 1160 G. Cathode gas flow rates of 3 to 30 cm^3/min STP of argon and helium were used, with a gas pressure of 3 to 10 mTorr in the cathode region and 0.2 to 3.0 mTorr in the diffusion chamber. A highly ionized column was obtained for arc current I_{arc} = 20 A. Cathode voltage with respect to the grounded anode was typically -40 V to -70 V in argon.

At each end of the 20-cm-diameter, 58.2-cm-long diffusion chamber, the axial boundaries consisted of 5 concentric end-ring electrodes, mounted on an alumina insulating plate. The inner two rings were quartered to provide information on azimuthal symmetry, as well as

to provide suitable suppressor electrodes for the application of linear feedback. All end-rings, the electrodes E_I, A_{II}, and E_{II}, and the diffusion region tank could be independently biased.

Langmuir probes were used as the primary diagnostic tool. All radial probes were inserted at the axial midplane. An axial probe could be rotated on its axis to provide axial plasma profiles at various radii and azimuths. A directional Langmuir probe (DLP), as discussed by Hudis and Lidsky, was employed in the present experiment to measure ion currents in the azimuthal and axial directions.[19] We tested the accuracy and reliability of the DLP by measuring directional currents in a microwave plasma device with a known streaming velocity.[20]

IV. RESULTS AND DISCUSSION

In the following experimental results, the electron temperature was obtained from a semilog plot of the probe I-V characteristic. The electron temperature falls off rapidly from ~3 eV near the central arc to less than 1 eV within 2 cm, and then decreases slowly to ~0.3 eV near the wall of the 20-cm-diameter diffusion chamber. The ion temperature was then calculated assuming heating by electrons and cooling by collisions with thermal neutral particles. The calculated ion temperature was in good agreement with the relation $T_i/T_e = 0.1$,[18] which is used in the calculations.

The plasma density falls from $\sim 10^{13}$ cm^{-3} near the central arc column to $\sim 10^{11}$ cm^{-3} near the wall. A flattening of the density profile exists in the region of large instability amplitude. This flattening has been correlated semiquantitatively with wave enhanced particle transport, comparable in magnitude with the Bohm value.[20]

When the axial end-ring boundaries are grounded to anode potential, a large, nonuniform, nonambipolar, radial electric field exists.

(Schwirzke argued that this field is caused by temperature gradients due to collisional cooling and by currents to the axial boundaries.[21]) A typical electric field profile, as determined using directional probe data, Eq. (14), is shown in Fig. 2 for the case of grounded end-rings. The electric field determined by this method is reproducible to better than 10%, and is in agreement with the value obtained from the slope of the plasma potential, $\phi_p = \phi_f + \gamma \frac{kT_e}{e}$ with $\gamma = (1/2)\ln(M_i/m_e) = 5.6$ for argon.

In this case, a low-frequency (LF $\approx$ 2 kHz) flute instability is observed at large radii in the region of large, positive electric field. The normalized wave amplitude is also shown in Fig. 2. The instability exhibits normal mode behavior in the sense that frequency is independent of position.

In order to compare theory with experiment, we use a "local" approximation rather than numerical integration over radial profiles for normal mode behavior. The basic assumption is that the wave properties are largely determined in regions where the destabilizing mechanisms are most important and, therefore, the wave amplitude is largest. It also allows us an analytic solution.

From Fig. 2 we see that the instability amplitude peaks in a rather broad radial range, extending over several centimeters. However, the plasma density, temperature, and radial electric field are also slowly varying in this region, so that the complex frequency, calculated from the dispersion relation using experimental profiles, is fairly uniform over the region of maximum wave amplitude.

With these approximations, rotational flute theory can predict several aspects of experimental instability behavior. Numerical solution of Eq. (6) yields the frequency and growth rate corresponding to local plasma conditions. There is, of course, no firm basis for comparing linear theory with wave amplitudes in nonlinear saturation. Nevertheless, the normalized temporal growth rate predicts (Fig. 2) that the wave will be most unstable near R = 6 cm. The large growth rate at larger radii is due to the steep density gradient near the wall. A rotationally driven, ion drift-type wave is predicted at higher frequency near the wall, but is not observed.

The growth rate for the instability was also measured directly using two independent techniques.[20] In one method the growth and decay rates were obtained by monitoring wave amplitudes on probes separated in azimuth, as the wave propagated azimuthally out of a region of negative and positive linear feedback, respectively. The wave amplitudes could be measured to ~15% accuracy. Also the amplitude was reduced by negative feedback to ~20% of its nonlinear saturation value, where linear theory is expected to be more valid. Agreement (±35%) between theory and experiment is obtained using this method for values of growth rate $\gamma/\Omega_r \lesssim 1$.

(Wave amplitude was also monitored temporally on a fixed probe after a stabilizing voltage on the axial boundaries was turned on or off. Accuracy was poor because large growth rates imply that the wave grows drastically in a single period so that exponential behavior is difficult

to determine. Better accuracy is predicted for lower growth rates, $\gamma/\Omega_r << 1.$)

The measured frequency versus the calculated local frequency, including Doppler shift due to plasma rotation, is shown in Fig. 3.

By measuring axial phase shifts with a PAR Model HR-8 lock-in amplifier, we could find no evidence for finite parallel wavelength. Phase measurement accuracy is specified as 5%, and uncertainty in azimuthal position of the axial probe is estimated to be ~15% for the worst case at small radii. We conclude that $\lambda_{||} > 24$ L, where L is the machine length. There is also no evidence for a standing wave in the axial direction.

Phase measurements from Langmuir probes at three azimuths, separated by 90° each, showed that the instability is an m = - 1 mode which propagates in the ion diamagnetic direction, in agreement with theory.

The phase by which the density leads the potential fluctuation is typically measured to be $\psi \simeq 150°$ to 170°, The phase calculated from Eq. (13), $\psi_{calc} \simeq 200°$ to 230°, is about 30% higher than experiment. For the case when collisional and Coriolis effects are important, Eq. (15) predicts $\psi \simeq 90°$ to 180°. When these effects are unimportant, Eq. (14) predicts $\psi = 180°$ to 270°. We note that the measured case lies between the two.

Rotational flute theory was also compared with other experiments under similar conditions. Hudis made frequency measurements in an HCD plasma, at similar neutral gas pressures, $p_0 \simeq 0.5$ mTorr Ar, but at larger magnetic fields.[7] With the anode at ground, and B = 1.82 kG, he measured a centrifugal flute instability peaked at radius R ≃ 4 cm

where $E_r \simeq 5$ V/cm. Using his parameters, we predict a Doppler shifted frequency of $f_{calc} = 3.2$ kHz, as compared with his measured value $f_{meas} \simeq 3.5$ kHz.

In another experiment with similar conditions, Ilić et al. observed an instability for B = 1.3 kG, but at lower pressure, $p_0 = 0.14$ mTorr Ar.[8] When their starting anode was grounded, they observed an m = - 1 instability, peaked near radius R = 2 cm in a region of positive electric field, $E_r \simeq 1$ V/cm. Using their data, we predict a frequency $f_{calc} = 11.5$ kHz, as compared with the measured value $f_{meas} = 7$ kHz. Their phase measurements are also similar to ours.

V. CONCLUSION

The present work adds new information regarding plasma stability based on simultaneous inclusion of most of the effects considered important in an HCD plasma. Examination of the resulting dispersion relation indicates that the Coriolis effect may be either stabilizing or destabilizing, depending on the direction of plasma rotation.[13] Ion-neutral collisions were found to be stabilizing both theoretically by varying the collision frequency in the dispersion relation, and experimentally by varying the neutral gas pressure. Collisions and the Coriolis force can also cause a significant shift in the phase between density and potential fluctuations.

A local, linear theory is obviously limited in its ability to explain the experimental behavior of normal modes in the nonlinear saturation limit. However, an analytic model does allow us to conclude that the effects of centrifugal and Coriolis forces due to plasma rotation are important regarding the stability of an HCD. We can predict several aspects of the

behavior of an instability observed in the present experiment, and also predict the frequency observed in two similar experiments.

Better quantitative agreement between theory and experiment will probably involve a complete fluid (or kinetic) description in cylindrical geometry, requiring numerical integration for normal mode behavior.

ACKNOWLEDGMENTS

This work was supported by the National Science Foundation and the U. S. Atomic Energy Commission.

REFERENCES

*Present address: Institute for Plasma Research, Stanford University, Stanford, California 94305

1. M. Kruskal and M. Schwarzschild, Proc. Roy. Soc. (London) 223, 348 (1954).

2. D. L. Morse, Phys. Fluids 8, 516 (1965); Phys. Fluids 8, 1339 (1965).

3. R. V. Aldridge and B. E. Keen, Plasma Phys. 12, 1 (1970).

4. G. X. Kambic, J. H. Noon and W. C. Jennings, Bull. Am. Phys. Soc. 16, 1236 (1971).

5. K. Chung and D. J. Rose, Bull. Am. Phys. Soc. 12, 694 (1967); Appl. Phys. Letters 11, 247 (1967).

6. R. L. Gunshor, J. H. Noon and E. H. Holt, Phys. Fluids 11, 1763 (1968).

7. M. Hudis, Ph. D. Thesis, Department of Nuclear Engineering, MIT, November 1969 (unpublished).

8. D. B. Ilić, T. D. Rognlien, S. A. Self and F. W. Crawford, Stanford University Institute for Plasma Research Report No. 482, July 1972 (submitted to Phys. Fluids).

9. F. F. Chen, Phys. Fluids 9, 965 (1966).

10. K. V. Roberts and J. B. Taylor, Phys. Rev. Letters 8, 197 (1962).

11. B. Lehnert, Phys. Fluids 5, 740 (1962).

12. W. B. Thompson, Reports on Progress in Physics (The Physical Soc., London, 1961), Vol. 24, p. 363.

13. P. D. Ariel and P. K. Bhatia, Nucl. Fusion 10, 141 (1970).

14. B. Lehnert, Phys. Rev. Letters 7, 440 (1961).

15. H. K. Hans, Nucl. Fusion 8, 89 (1968).

16. F. F. Chen, Phys. Fluids 8, 912 (1965).

17. L. M. Lidsky, S. D. Rothleder, D. J. Rose, S. Yoshikawa, C. Michelson and R. J. Mackin Jr., J. Appl. Phys. 33, 2490 (1962).

18. M. Hudis, K. Chung and D. J. Rose, J. Appl. Phys. 39, 3297 (1968).

19. M. Hudis and L. M. Lidsky, J. Appl. Phys. 41, 5011 (1970).

20. G. M. Wheeler, Lawrence Berkeley Laboratory Report No. LBL-577, January 1972 (unpublished).

21. F. Schwirzke, Phys. Fluids 9, 2244 (1966).

FIGURE CAPTIONS

Fig. 1. Hollow cathode arc discharge experiment.

Fig. 2. Radial electric field, O, as determined using a directional Langmuir probe is reproducible to better than 10%. Also shown is normalized instability amplitude, Δ, $\tilde{n} \equiv n_1/n_0$, LF = 1.83 kHz; and calculated normalized growth rate, □, $\gamma/\Omega_r \times 10^{-1}$, where $\omega = \Omega_r + i\gamma$. p_0 = 0.25 mTorr Ar, B = 580 G.

Fig. 3. Measured vs. calculated frequency. x, argon, B = 580 G; O, argon, B = 870 G; O, argon, B = 1160 G; Δ, helium, B = 580 G; ∇, helium, B = 870 G; □, helium, B = 1160 G.

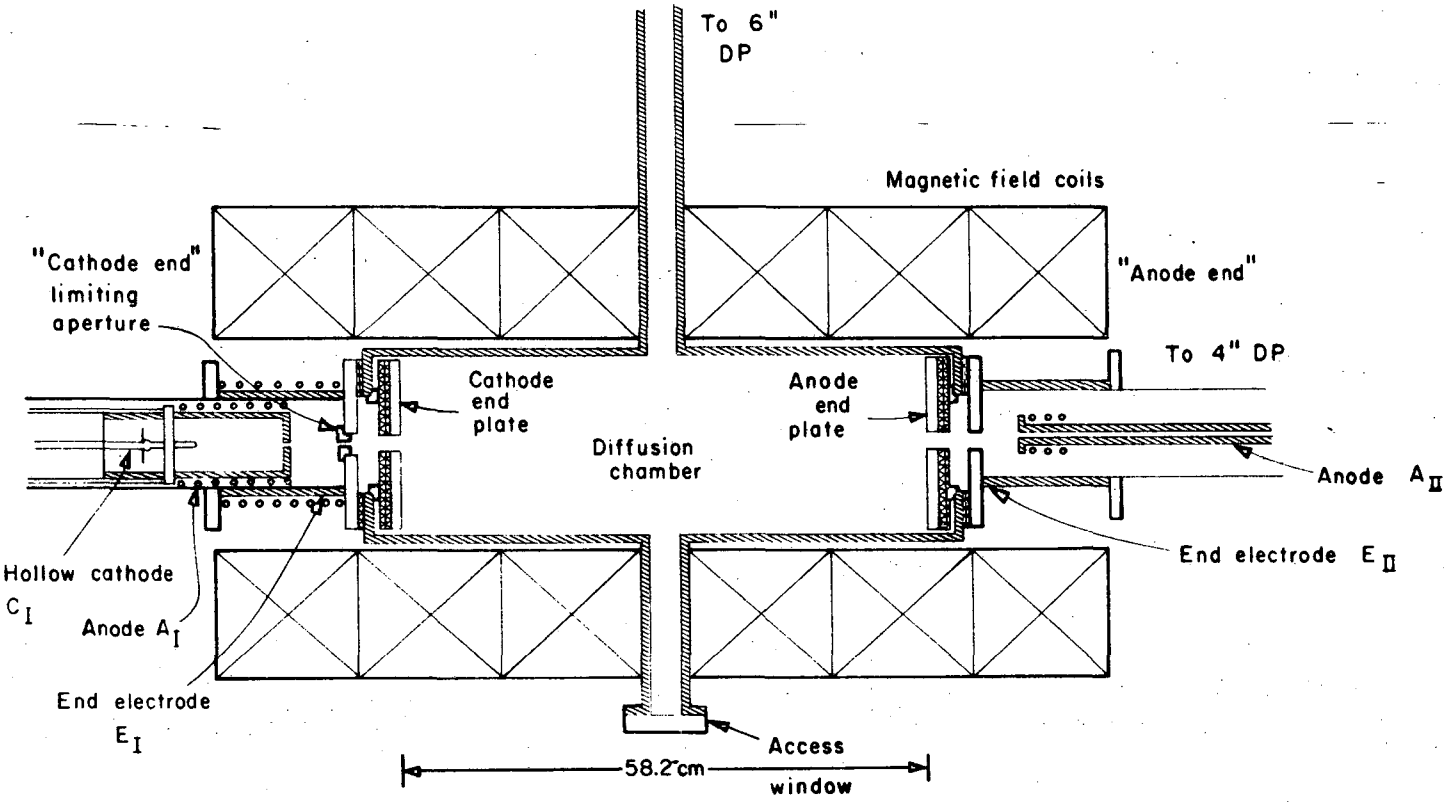

XBL676-3255

Fig. 1

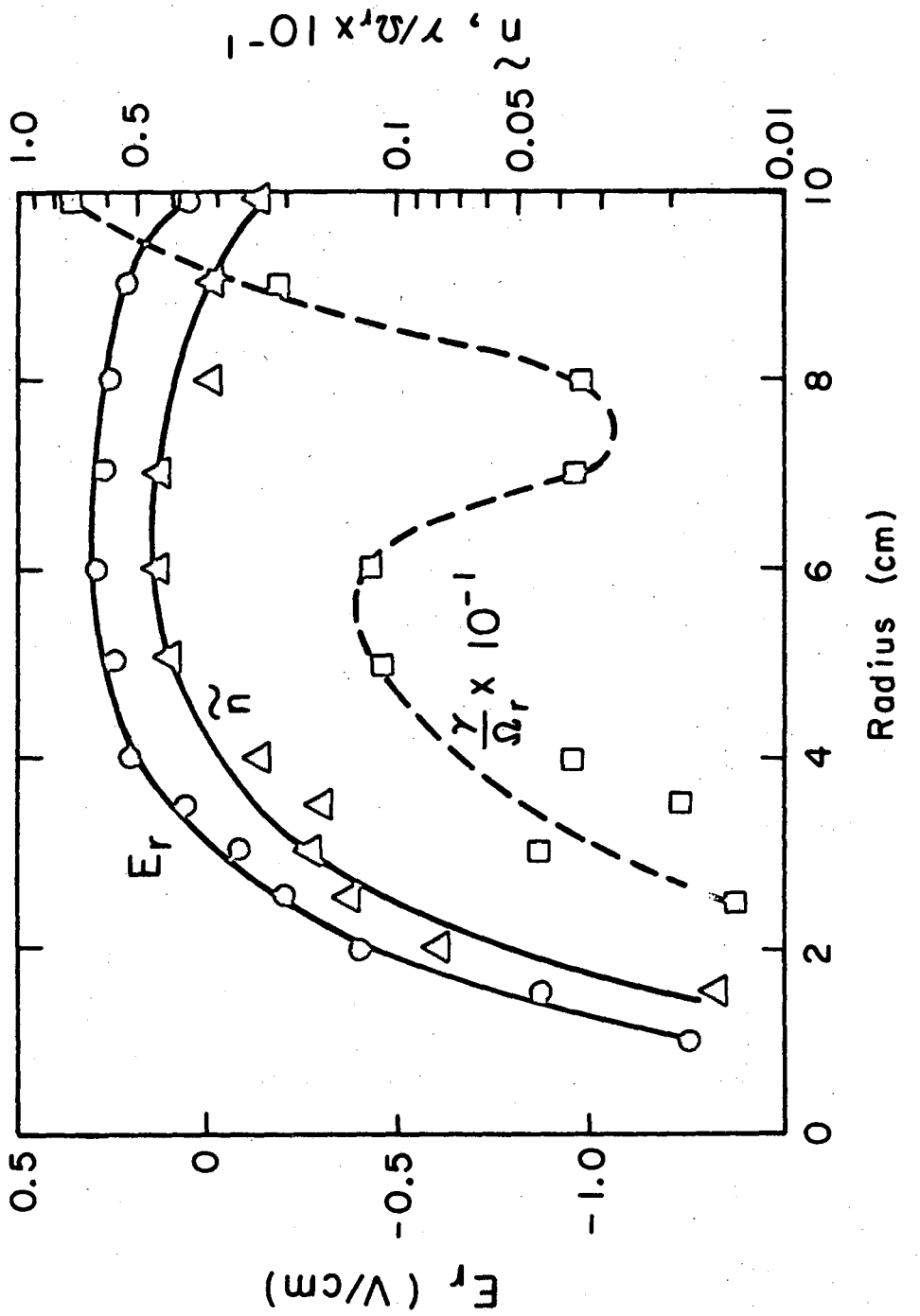

XBL735-2809

Fig. 2

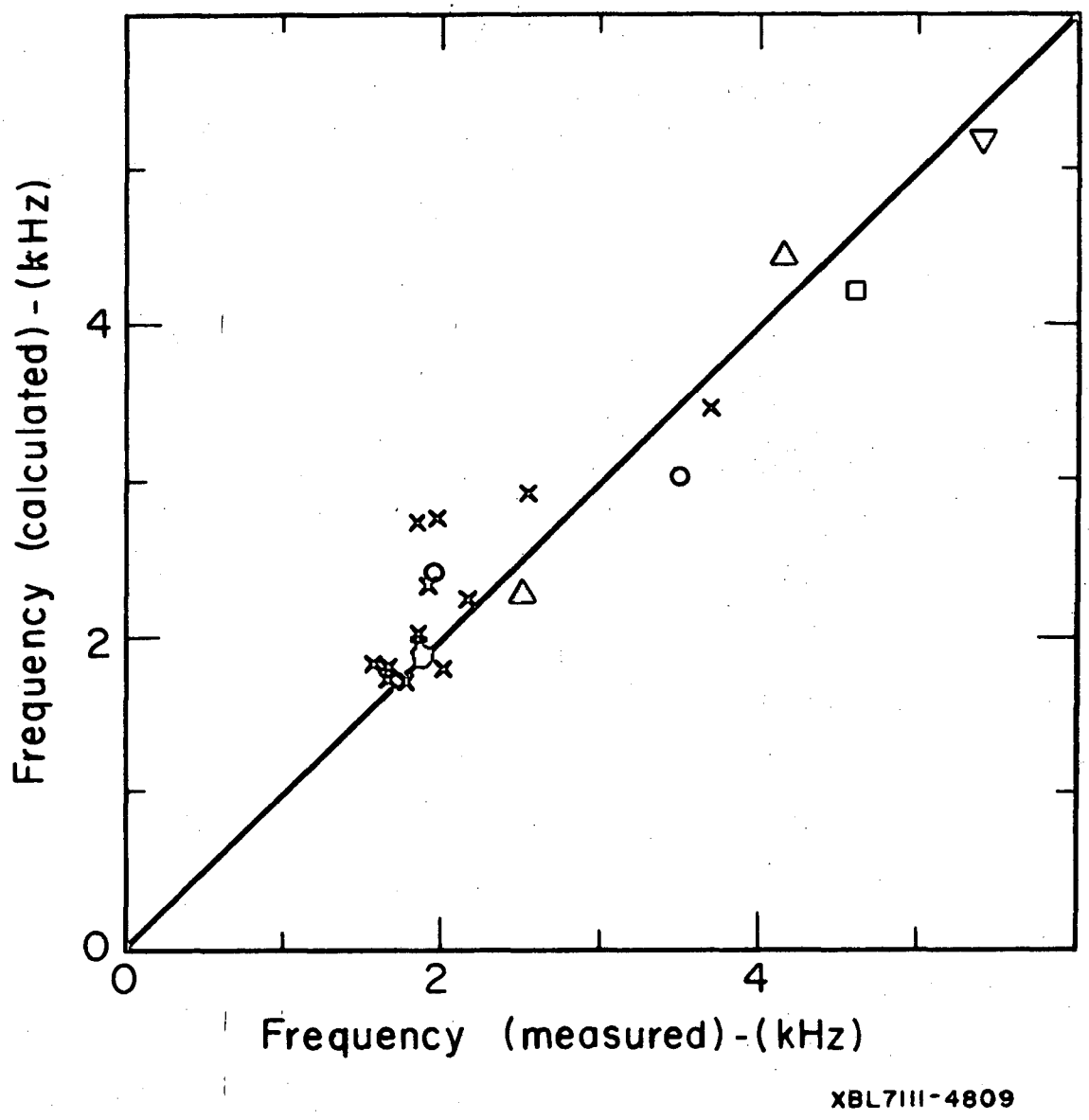
Frequency (calculated) - (kHz)
Frequency (measured) - (kHz)
0
2
4
0
2
4
XBL7111-4809

Fig. 3

TECHNICAL INFORMATION DIVISION
LAWRENCE BERKELEY LABORATORY
UNIVERSITY OF CALIFORNIA
BERKELEY, CALIFORNIA 94720